S V E N S K A G E O F Y S I S K A F Ö R E N I N G E N

VOLUME 10, NUMBER 1 Tellus FEBRUARY 1958

A QUARTERLY JOURNAL OF GEOPHYSICS

Vertical Circulation and Release of Kinetic Energy during the Development of Hurricane Hazel into an Extratropical Storm

By E. PALMÉN, Academy of Finland

(Manuscript received June 5, 1957)

Abstract

The thermal structure of the atmosphere over the eastern and central parts of the U. S. on October 15, 1954, when the tropical hurricane "Hazel" entered the American continent and rapidly was transformed into an extratropical cyclone of great intensity, is analyzed by the aid of upper air charts and vertical cross sections. The field of divergence and vertical velocity is determined from the horizontal wind field at different levels for the synoptic time October 15, 1500 GCT, and the results are used for computing the precipitation in the region of strongest ascent of the warm and moist air of the tropical disturbance and for a determination of the release of kinetic energy in the whole region due to vertical solenoidal circulations associated with the general sinking of the cold polar air masses and the simultaneous ascent of the warm tropical air masses. The production of kinetic energy is also computed directly from the work done by the horizontal pressure forces in the same area. Both methods give a production of kinetic energy of about 19×10^{10} kilojoules or 19×10^{20} ergs per second over an area 366×10^4 km^2 large. Only a small part of the energy released is again dissipated due to friction in the same area, whereas the essential part is exported outwards from the source region, thus furnishing the surrounding atmosphere with large amounts of kinetic energy.

In the last section some general conclusions are made concerning the budget of kinetic energy in the whole Northern Hemisphere, considering the net effect of the disturbances in the westerlies, the mean meridional circulations, the mean meridional flux of kinetic energy and the frictional dissipation.

1. Introduction

The unusual behavior of the tropical cyclone "Hazel" (October 1954) over the North American continent has been discussed by KRUEGER (1954), MOOK (1955), DAVIS (1954), KNOX (1955) and by HUGHES, BAER, BIRCHFIELD and KAYLOR (1955). In these papers the unusual path of the cyclone over the U.S. mainland, the acceleration of the movement and the rapid change of the storm, from a typical tropical cyclone into an extratropical disturbance of great intensity, were attributed to the simultaneous wave pattern of the upper air flow in the extratropical westerlies. Due to a rare coincidence a strong extratropical development occurred over the eastern parts of the U.S., and the tropical cyclone became rapidly absorbed into this new development, with the result that the decay that normally occurs when tropical cyclones move inland did not happen in this case.

As was pointed out by Knox the rapid change of "Hazel" from a tropical into an extratropical storm occurred between October 15, 1500 GCT and October 16, 0300 GCT. In the present study only this stage of the development will be subjected to a detailed analysis. The synoptic situation and the development of the extratropical cyclone "Hazel" during this time of transition are in many respects of general interest, since the case offers an opportunity for the comparison of tropical and extratropical storms with respect to their sources of energy. On account

1—709370

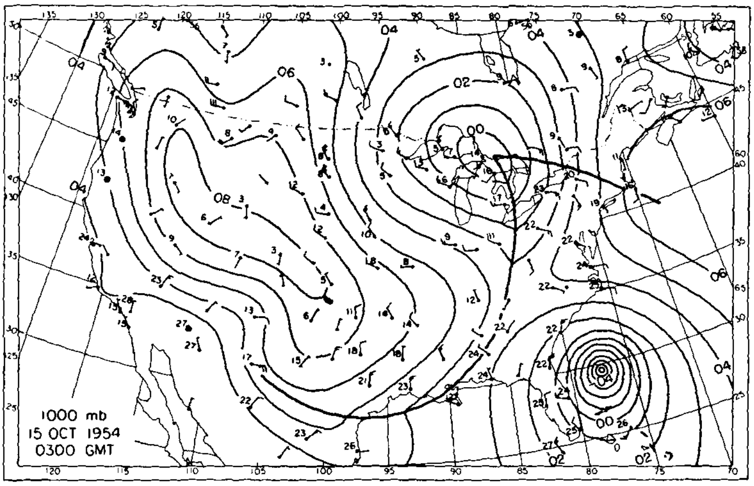

Fig. 1.

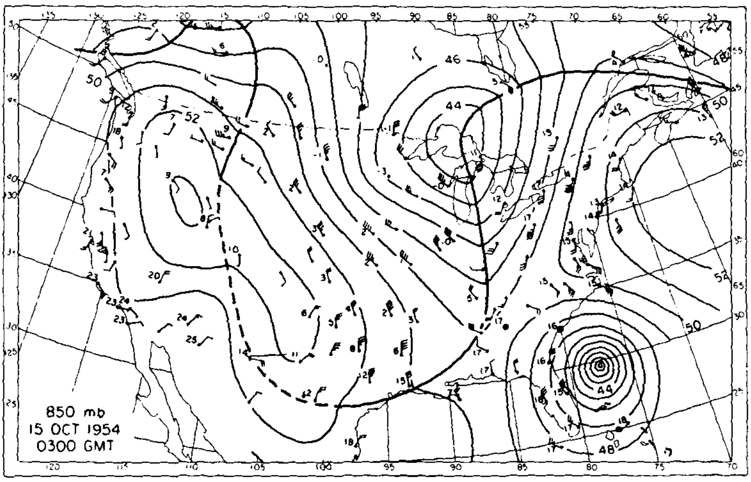

Fig. 2.

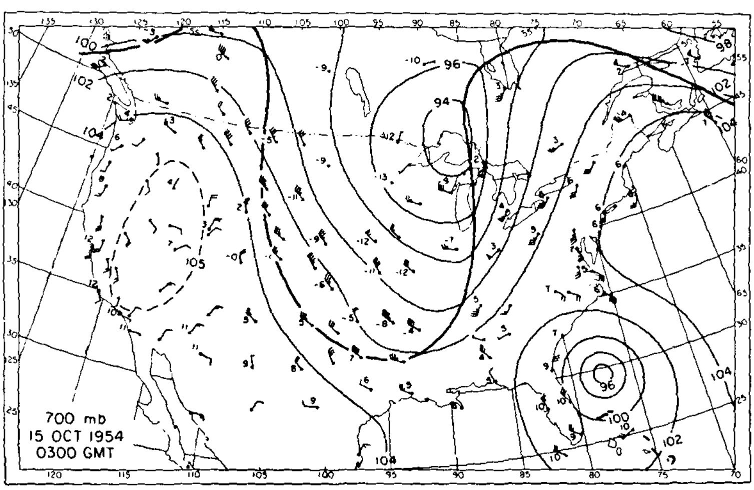

Fig. 3.

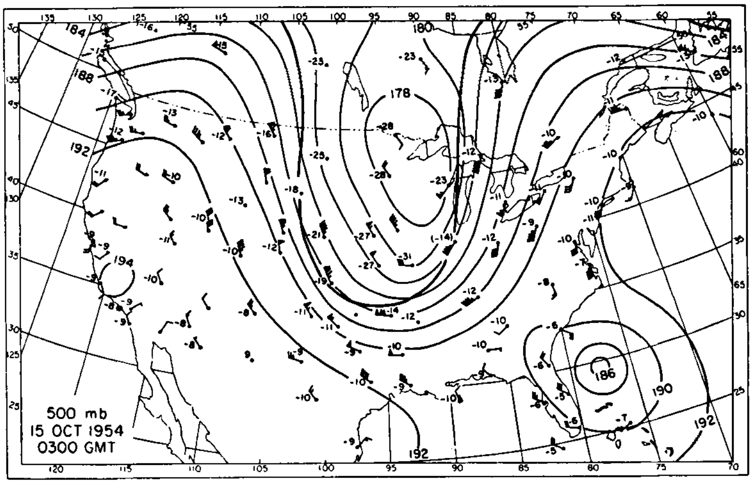

Fig. 4.

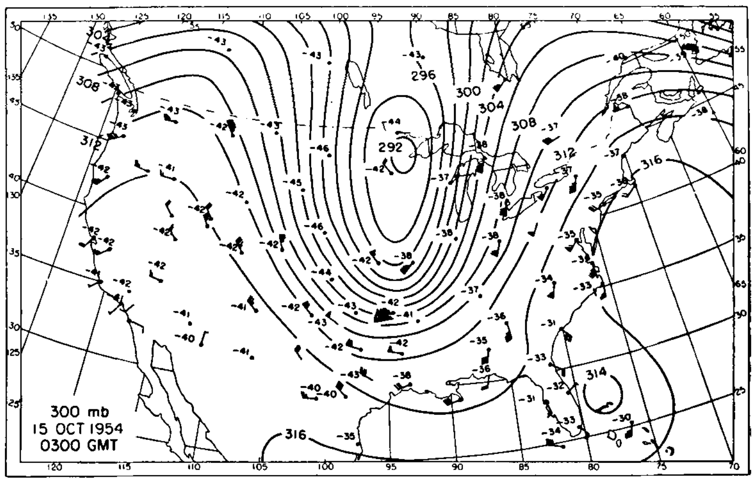

Fig. 5.

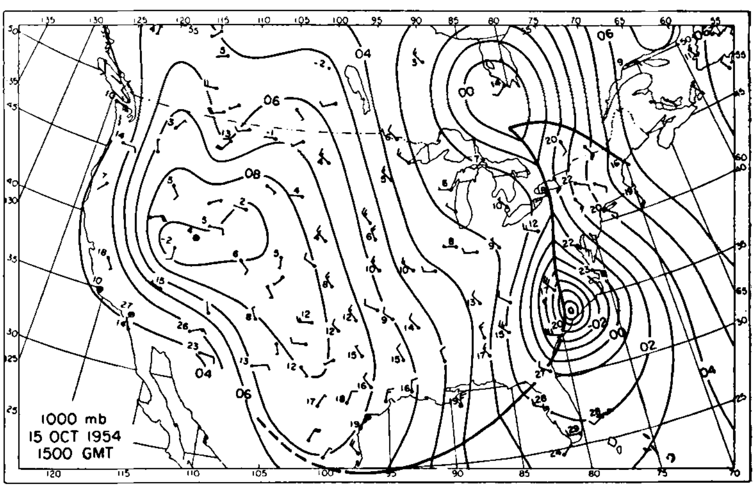

Fig. 6.

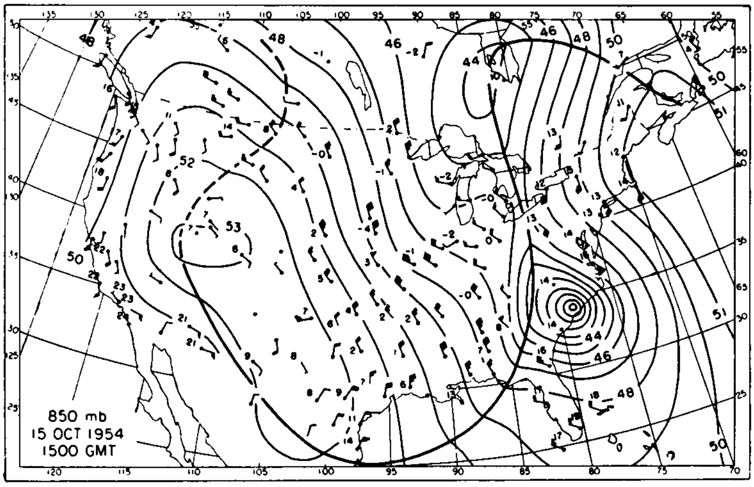

Fig. 7.

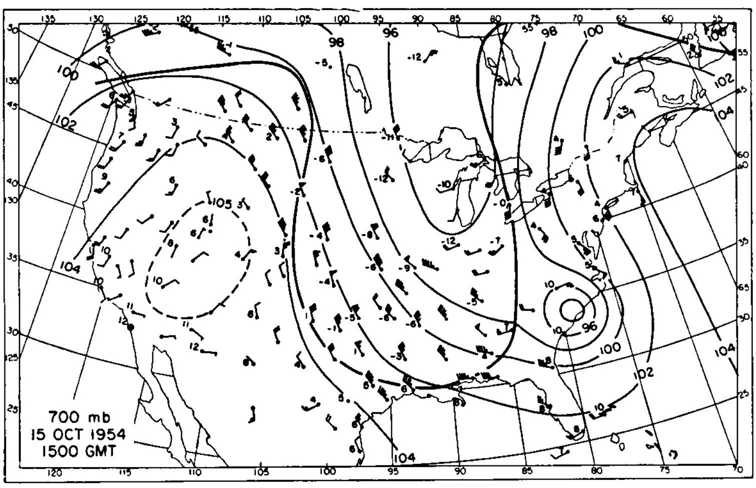

Fig. 8.

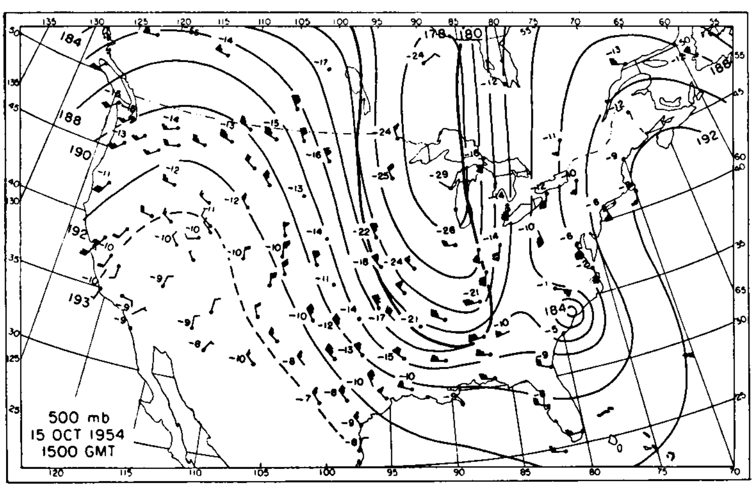

Fig. 9.

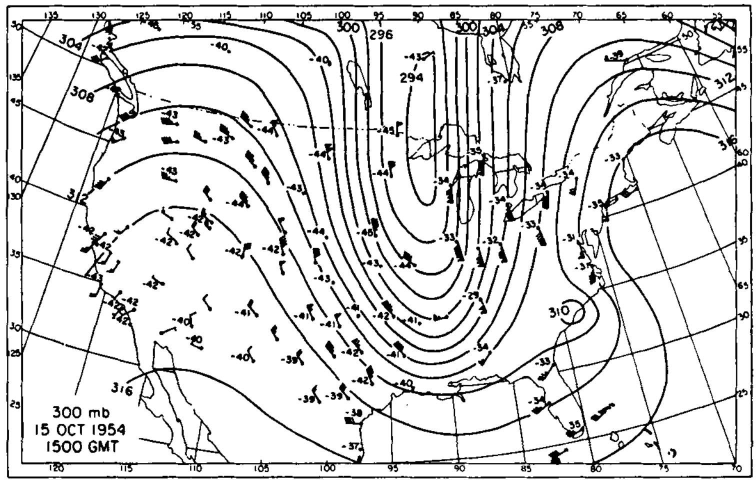

Fig. 10.

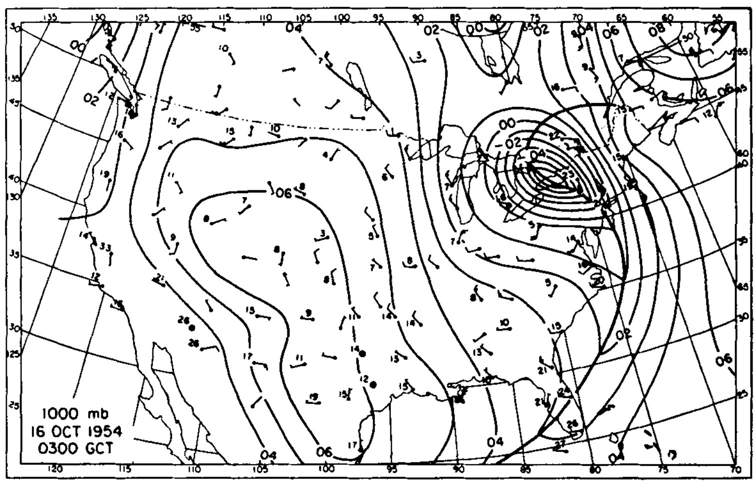

Fig. 11.

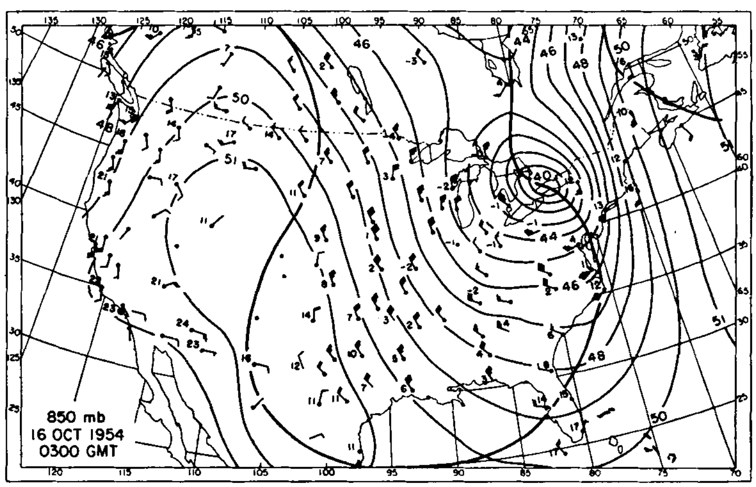

Fig. 12.

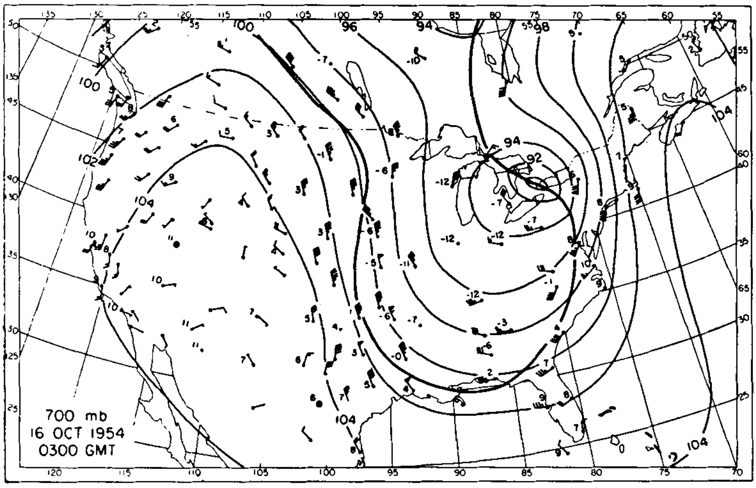

Fig. 13.

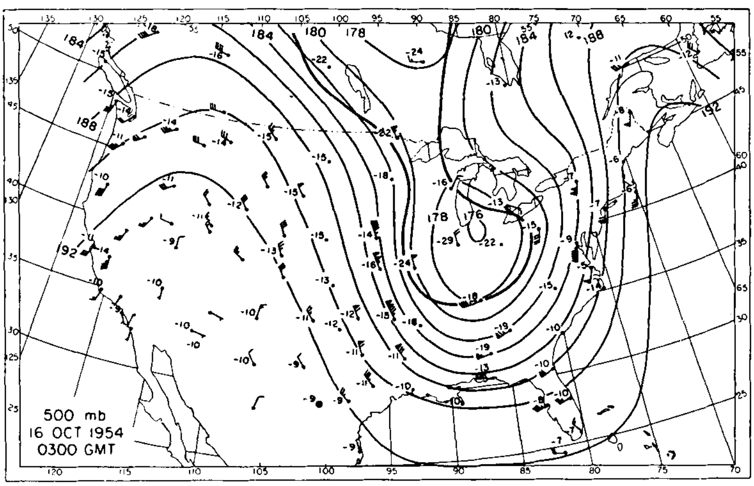

Fig. 14.

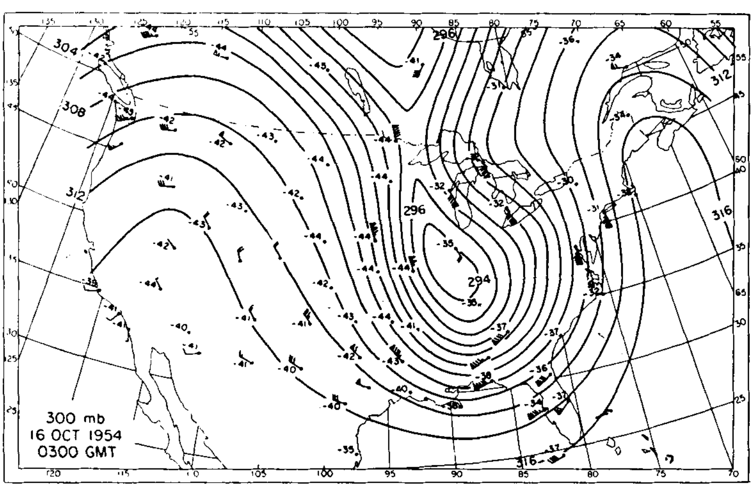

Fig. 15.

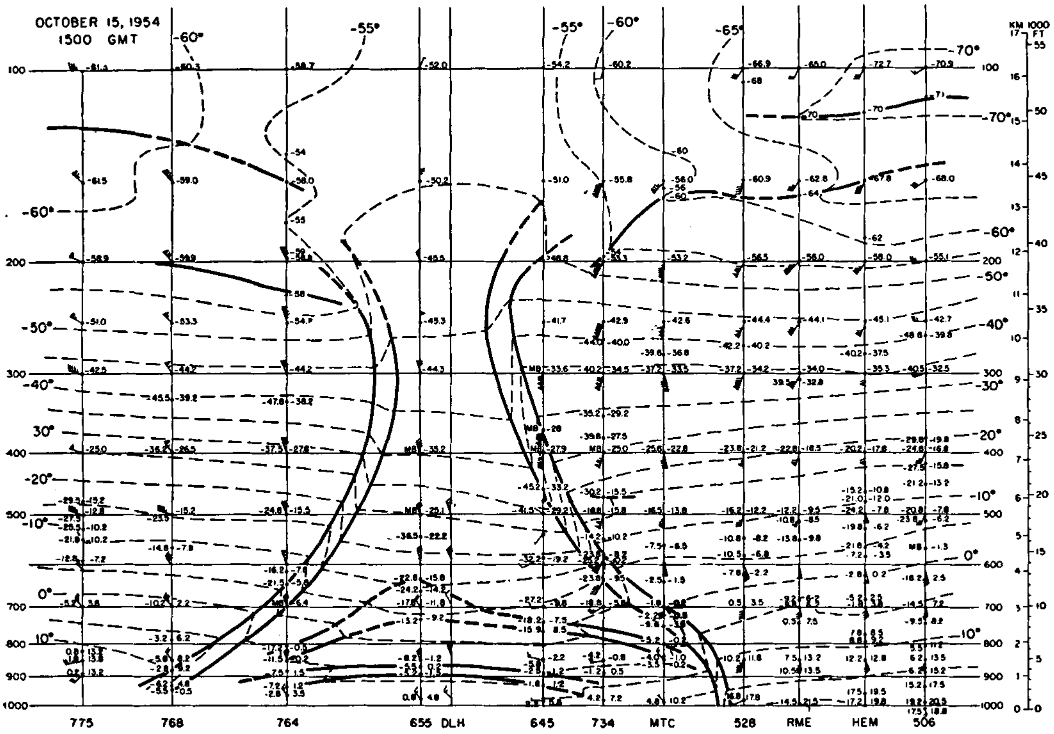

Fig. 16. Vertical cross-section, October 15, 1500 GCT, approximately along parallel 45° N. Thin dashed lines are isotherms, and heavy lines frontal boundaries, inversions or tropopauses. Temperature, dewpoint and wind are indicated at standard levels and significant points.

of the unusual path of the storm, a large number of upper air stations could be used, both for the synoptic analyses and for different kinds of computations.

The principal aim of the investigation was to determine directly from the observed winds and pressures the field of divergence, the vertical velocity, and the release of kinetic energy due to vertical solenoidal circulations. The synoptic time, October 15, 1500 GCT, was selected for the experiment because the principal development at that time occurred in a region with a relatively dense network of upper air stations. An extension of the experimental investigation to other synoptic times would have been very desirable; however, due to the sparseness of aerological stations over the Atlantic Ocean and over eastern Canada, the results would hardly have been satisfactory.

2. Synoptic Situation

In Figs. 1—15 the synoptic charts for the 1,000, 850, 700, 500 and 300 mb surfaces for October 15, 0300, 1500 and October 16, 0300 GCT are reproduced. The charts contain only temperatures, winds, contour lines and the principal fronts. By principal fronts is here meant a boundary separating the warm air from a frontal zone of finite thickness in regions where the front was sufficiently distinct. Concerning details of the surface maps the readers are referred to aforementioned investigations of cyclone "Hazel".

As can be seen from the charts an intense cold front approached the tropical storm "Hazel" when it moved in over the U.S. mainland around October 15, 1500 GCT. The cold air mass to the west and the northwest was of great depth and reached to the tropopause level along a tongue extending from

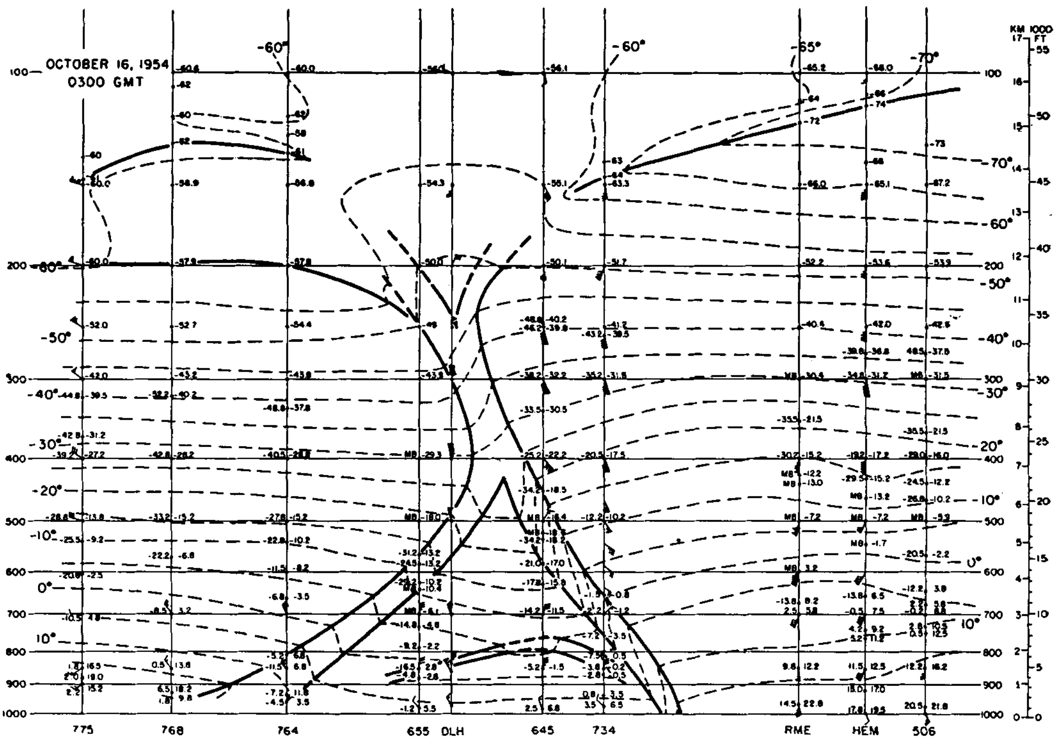

Fig. 17. Vertical cross section, October 16, 0300 GCT, approximately along parallel 45° N. Symbols as in Fig. 16.

northern Canada southward to about 38° N. At the 500 mb level, temperatures in the range from -27 to -31° C were found on October 15, 0300 GCT, as far south as 38° N, which is unusually cold for this time of the year. The temperature contrasts between the two principal air masses were extremely large; at the 500 mb level differences as large as 15° C were found in the vicinity of the cold front, with an over-all contrast of 25—28° C between the cold trough and the tropical air over the cyclone.

The thermal structure of the atmosphere is shown in greater detail in two vertical cross sections approximately along latitude 45° N for October 15, 1500 GCT and 16, 0300 GCT (Figs. 16 and 17). The cold air of polar origin is well distinguished from the surrounding warmer air masses. Especially the eastern boundary is extremely well marked. Here the frontal boundary can be followed up to levels where the temperature difference between the principal air masses normally vanishes. In the present case the front at these upper levels is still marked by very strong horizontal wind shear.

Twelve hours later the western warm air in the same zonal cross section has reached the eastern warm air above the 430-mb level, thus forming a pronounced zone of strong horizontal wind shear with the characteristics of an occluded front in the upper troposhere and in the tropopause region. In this respect the development was similar to the occlusion process associated with the strong cyclogenesis in November, 1950 (Palmén, 1953).[1] At lower levels the cold air was still well distinguished from the surrounding warm air, as can be seen from Fig. 17.

[1] The essential difference between the synoptic situation on October 15, 1954 and on November 25, 1950 was that in the latter case no tropical storm existed prior to the development. In spite of this the general development showed great similarities.

The frontal contours at the 500-mb level for four consecutive synoptic times are presented in Fig. 18. The figure shows the movement and deformation of the cold tongue during the period October 14, 1500—16, 0300 GCT. In spite of a net flow of cold air southwards across latitude circles (e.g., 50° or 45° N) the area occupied by the cold air decreased, indicating a general subsidence inside the cold mass (PALMÉN and NEWTON, 1951).

A more detailed picture of the temperature and wind fields on both sides of the cold front over the eastern part of the U.S. is given in Fig. 19. In this zonal cross section, approximately along latitude 40° N, three radiosonde stations and, in addition, one wind station show the characteristic change of temperature and wind in the soundings penetrating the frontal layer. Both the temperature contrast and the wind shear reach maximal values in the upper troposphere, between 500 and 300 mb. Around 400 mb

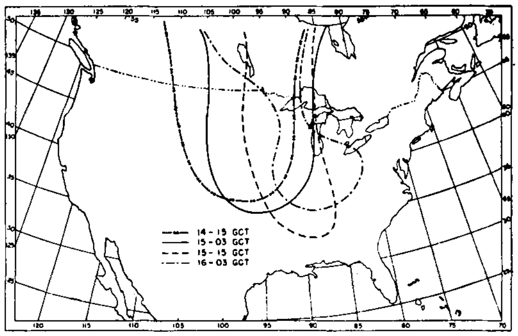

Fig. 18. Frontal contours at the 500-mb surface on October 14, 1500 to October 16, 0300 GCT.

the wind changes from W 30 kts to SSE 140 kts through a vertical distance of about 1.6 km across the front, corresponding to an increase of the wind component normal to the cross section of about 72 m sec^{-1}. The temperature field inside the frontal layer gives a corresponding value of 65 m

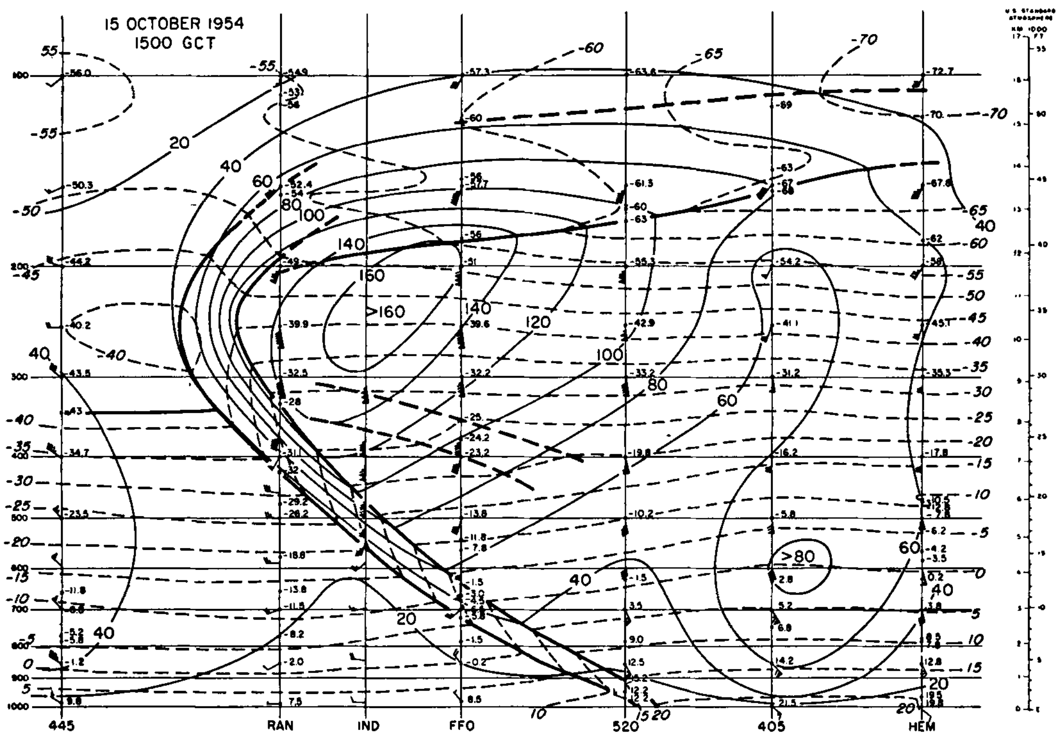

Fig. 19. Vertical cross-section, October 15, 1500 GCT, approximately along parallel 40° N. Thin dashed lines are isotherms, and heavy lines mark frontal boundaries or tropopauses. The thin solid lines mark isotachs at intervals of 20 kt of observed wind, without regard to direction.

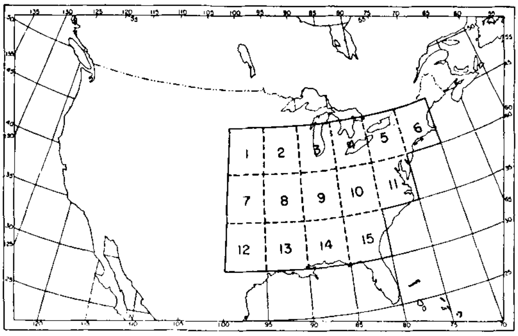

Fig. 20. The 15 different blocks used in the computations.

sec^{-1} as the increase of the geostrophic component normal to the cross section.

The cross section shows a wind maximum of more than 160 kts around 250 mb, almost vertically above the intersection between the frontal layer and the 500-mb surface. A second layer with pronounced vertical stability and a secondary maximum in the vertical wind shear is indicated by dashed lines between 400 and 300 mb. This ascendary boundary, with a slope less than that of the principal front, seems to separate the almost saturated air aloft from the dryer warm air below. Cloud observations indicate that this upper warm air with high moisture content represents the upper outflow from the region of the rapidly ascending motion in the rain area of the storm. The separate wind maximum of 80 kts around station 405 belongs to the tropical storm.

A radical change in the thermal structure of the cyclone occurred during the 12-hour period from October 15, 1500 to October 16, 0300 GCT. At the former time the center of the tropical cyclone was still well marked as a warm depression throughout the troposphere, but 12 hours later the tropical cyclone was completely amalgamated with the large extratropical disturbance, so that no sign of the previously existing separate center of circulation associated with the tropical cyclone can be distinguished at any level. Both at low and high levels the thermal structure shows the characteristics of a typical extratropical cyclone with its asymmetric temperature distribution.

The temperature field in the upper troposphere shows some interesting features during the period from October 15 to 16. During this period of the development an unusually warm mass of air with high dewpoint temperatures, indicating saturation or supersaturation in respect of ice, spread out at the 300 and 200 mb levels over the region of the Great Lakes and southeastern Canada.[2] The potential wet-bulb temperature of this upper air equalled that of the surface layer over the ocean to the southeast of the American continent, whereas the air at the same levels to the west of the upper trough was considerably colder. The analysis shows that this warm and moist air could not have been brought around the upper trough, but was oceanic tropical air which had been lifted from the surface layers in the central parts of the tropical cyclone.

3. Computation of Divergence and Vertical Velocity

For the computation of the divergence field and vertical velocity on October 15, 1500 GCT, the area indicated in Fig. 20 was used. The total area was divided into 15 different blocks, each being five degrees latitude and

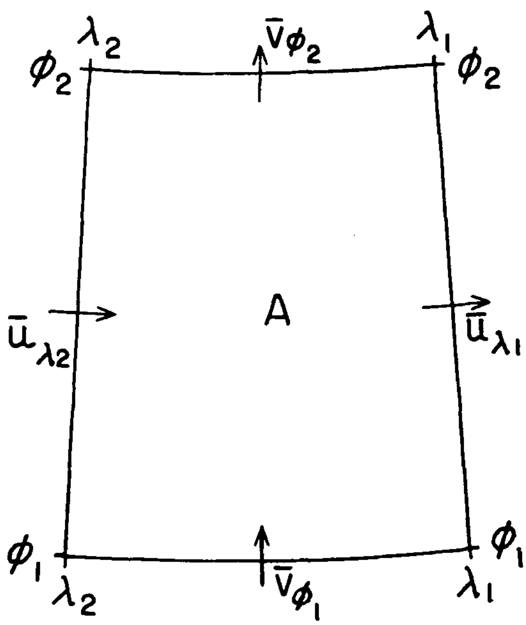

Fig. 21. Schematic picture of a block and the mean values of zonal and meridional wind components used for the computations of divergence.

[2] The dewpoint temperatures have not been plotted in the charts and cross-sections.

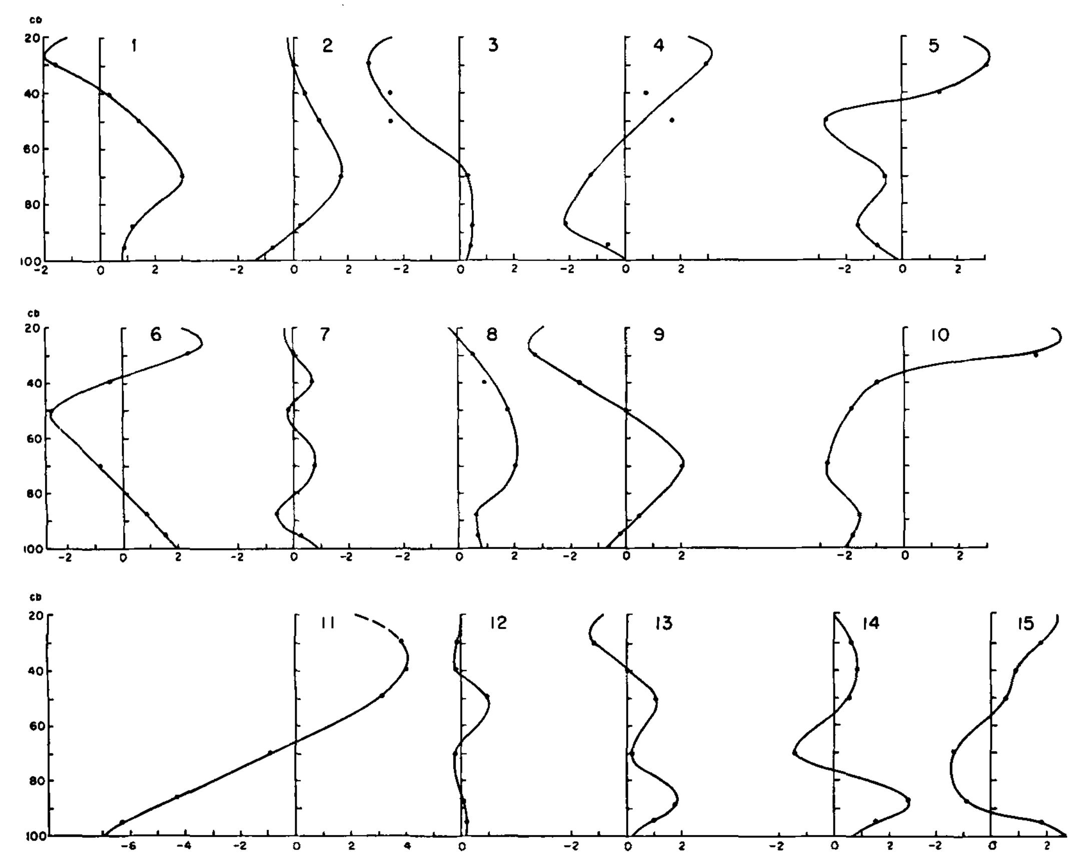

Fig. 22. Distribution of the mean divergence as a function of pressure in the 15 different blocks of Fig. 20. Unit: 10^{-5} sec^{-1}.

longitude. For each block the divergence was determined from the formula.

$$\int_{A_i} \nabla_H \cdot \mathbf{v}\,\delta A = \int_{L_i} v_n\,\delta L \qquad (1)$$

where A_i denotes the area of the block, L_i the length of its boundary, and v_n the wind component along the exterior normal of the boundary. If the bar denotes the mean value over the area, or over the boundary, respectively, the mean divergence at an arbitrary level is given by

$$\overline{\nabla_H \cdot \mathbf{v}} = \frac{L_i}{A_i}\overline{v_n} \qquad (2)$$

For the practical computation the following formula was used (see Fig. 21)

$$L_i \overline{v_n} = a(\varphi_2 - \varphi_1)(\overline{u}_{\lambda_1} - \overline{u}_{\lambda_2}) + a(\lambda_2 - \lambda_1)(\overline{v}_{\varphi_2} \cos \varphi_2 - \overline{v}_{\varphi_1} \cos \varphi_1) \qquad (3)$$

Here $\overline{u}_\lambda$ and $\overline{v}_\varphi$ denote the mean zonal and meridional wind components at the sides of the block, φ and λ signify latitude and longitude, and a denotes the radius of the figure of the earth.

For the determination of the mean wind components special wind charts were plotted for the 2,000, 4,000, 10,000, 18,000, 23,000 and 30,000 ft. levels, corresponding approximately to 940, 870, 700, 500, 400 and 300 mb. On these charts component isotachs were drawn, and the values for $\overline{u}_{\lambda_1}$, $\overline{u}_{\lambda_2}$, and $\overline{v}_{\varphi_1}$, $\overline{v}_{\varphi_2}$, were computed. The analysis of the original wind field was extended to a somewhat larger area than that indicated in Fig. 20.

The accuracy of these determinations depends essentially upon the number of stations and the quality of the observed winds. Most meteorologists who have tried to compute the divergence field from actual wind observa-

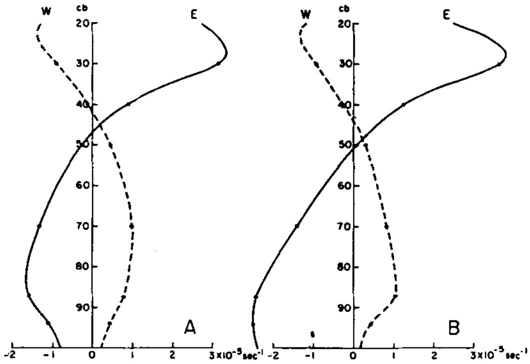

Fig. 23.
A: Mean divergence in 9 western blocks and in 6 eastern blocks.
B: Mean divergence in 6 western blocks and 4 eastern blocks.

tions have found the method rather unsatisfactory due to numerous errors and local deviations in the observed winds. In the case discussed here the divergence was expected to be relatively large since strong development was involved. It is reasonable, therefore, to assume that the errors would not substantially distort the large-scale divergence patterns.

The result of the computations for each of the 15 blocks in Fig. 20 is presented in Fig. 22 which gives the divergence as a function of pressure. At a first glance at the different curves the results do not appear very satisfactory because of numerous irregularities of a type obviously caused by errors in the original wind data or in the isotachs analyses. One exception can be seen in block 11 where the distribution of the divergence is very regular, with large negative values in the lowest layers and large positive values above about 600 mb. This block covers most of the region of heavy precipitation in the most active part of the tropical cyclone, where the divergence necessarily must reach extreme values.

A considerably more satisfactory picture results, however, if mean values of the divergence are determined for larger areas. If the total area in Fig. 20 is divided into two parts, a western and an eastern area separated by the meridian 85 W, the western part is essentially covered by cold polar air masses, at least up to the middle of the troposphere, while the eastern part, from the layer 1,000—700 mb and upwards, is occupied by warm air masses. Fig. 23 A gives the distribution of the mean divergence in the two different regions, with 9 of the blocks in Fig. 20 in the western region and 6 of the blocks in the eastern region. In the western region (i.e., the region of cold air) the mean divergence is positive in the lower layers up to around 415 mb with convergence above that level, while in the eastern part the lower layers up to 465 mb is characterized by convergence and the layers above 465 mb by divergence. The mean level of non-divergence is around 440 mb. The upper divergence in the eastern part is large, reaching values of about 3.2×10^{-5} $\sec^{-1}$ at the 300-mb level.

Both the horizontal and vertical distribution of the divergence correspond closely to the picture presented by PETTERSSEN and BRADBURY (1954) for another case of strong development (November 23—27, 1952). In their case, however, the divergence field was computed from the geostrophic vorticity field.

The characteristic difference between the behavior of the cold and warm air is still clearer if some of the blocks in Fig. 20 are excluded. In Fig. 23 B, the mean divergence for the 6 western blocks (Nos. 2, 3, 8, 9, 13, 14) and the 4 eastern blocks (Nos. 4, 5, 10, 11) is presented. The eastern group now contains essentially the region of precipitation or the area covered by the upper cloud sheet which extended from the active part of the cyclone, while the western part is occupied by cold air up to high altitudes. The mean level of non-divergence is now around 470 mb, with pronounced convergence (2.5×10^{-5} $\sec^{-1}$) in the surface layers of the rain and cloud area and a very strong upper divergence (with maximum values of 4×10^{-5} $\sec^{-1}$) around or just below the tropopause level.

From the equation of continuity one obtains

$$\Big[\varrho w\Big]_{H_1}^{H_2} = -\frac{1}{g}\int_{p_2}^{p_1} \nabla_H \cdot \mathbf{v}\,\delta p - \int_{H_1}^{H_2}\left(\frac{\partial \varrho}{\partial t} + \mathbf{v}\cdot\nabla_H \varrho\right)\delta z \qquad (4)$$

where ϱ is the density, w the vertical wind component, g the acceleration of gravity,

Table 1. Mean vertical velocity (cm sec^{-1}) in the different blocks

	Isobaric surfaces, mb						
Block	900	800	700	600	500	400	300
1	−0.7	−2.4	−5.2	−9.8	−14.4	−19.0	−22.1
2	0.6	0.1	−1.2	−3.4	−5.8	−8.0	−10.6
3	−0.4	−0.8	−1.1	0.3	2.4	7.1	16.5
4	0.8	3.0	5.4	7.2	6.7	6.2	2.4
5	0.7	2.4	3.5	5.6	10.2	14.4	12.8
6	−1.3	−2.3	−2.0	−0.5	2.8	6.0	5.9
7	−0.2	0.1	−0.2	−1.2	−1.3	−2.0	−3.5
8	−0.6	−1.4	−3.6	−6.6	−10.4	−15.1	−21.6
9	0.2	−0.6	−2.4	−5.0	− 6.6	−6.6	−3.0
10	1.5	3.6	7.2	11.6	16.8	23.0	27.6
11	5.9	10.3	13.1	14.7	13.7	9.4	2.6
12	−0.2	−0.1	−0.4	0.1	−1.0	−1.8	−1.8
13	−0.8	−2.2	−3.4	−4.3	−6.8	−9.2	−10.6
14	−1.4	−3.6	−4.2	−3.2	−4.0	−6.4	−9.8
15	−1.2	−0.1	1.2	2.7	2.6	2.1	−0.1
Mean	0.2	0.4	0.5	0.5	0.3	0.0	−1.0

and $\nabla_H \cdot \mathbf{v}$ and $\nabla_H \varrho$ are the horizontal divergence and density ascendant, respectively. The equation gives the difference in ϱw between two arbitrary levels H_1 and H_2 with the corresponding pressures p_1 and p_2. The last term in Eq. (4) can be considered to be small as compared with the divergence term. If it is neglected and if w is assumed to be zero at the ground, or approximately at p = 1,000 mb, one obtains the values of the vertical velocity shown in Table 1.

The mean values over all of the 15 blocks indicate a slight mean convergence in the lowest atmospheric layers and divergence above 700 mb. Whether this mean divergence field is real or the result of an accumulation of different errors is difficult to decide.

If the vertical velocities are combined in the manner shown in Fig. 23, into a western and eastern group separated by the meridian 85° W, one obtains the mean values given in Table 2.

Since the western groups essentially represent the cold air to the west of the front at the level 700—600 mb and the eastern groups represent the warm air to the east of the front, Table 2 shows that, on the average, the warm air is ascending and the cold air descending, resulting in an energy producing vertical circulation. This mean vertical circulation was essentially in a zonal direction.

4. Precipiation and Divergence Field

The precipitation pattern during the period from October 15 to 16 shows clearly the rapid amalgamation of the tropical cyclone "Hazel" with the large extratropical disturbance which developed over the eastern part of the American continent. At the beginning of the period two separate rain areas could be distinguished, but already on October 15, 1500 GCT both areas were combined into an elongated rain band essentially along the front, with maximum intensity just west of the surface front.

Table 2. Mean vertical velocity (cm sec^{-1}) in the 9 or 6 western blocks and in the 6 or 4 eastern blocks.

	Isobaric surfaces, mb						
Group	900	800	700	600	500	400	300
9 W	−0.5	−1.2	−2.4	−3.6	−5.6	−6.8	−7.4
6 E	1.1	2.8	4.7	6.9	8.8	10.2	8.5
6 W	−0.4	−1.4	−2.7	−3.7	−5.2	−6.4	−6.5
4 E	2.2	4.8	7.3	9.8	11.9	13.2	11.3